Studying of 2,2′-Bipyrimidine Based Dyes Properties as Photo-Sensitizer for Dye Sensitized Solar Cells (DSSCs)

S. Krishnaveni[1,], X. Mary Josephine[2,] and V. Sathyanarayanamoorthi[1,*,]

[1]Department of Physics, PSG College of Arts and Science, Coimbatore-641014, India
[2]Department of Physics, Nirmala College for Women, Coimbatore-641018, India

*Corresponding author: E-mail: sathyanarayanamoorthi@psgcas.ac.in

In this investigation, five novel π-new organic donor-π-acceptor dyes (D-π-A) based on 2,2′-bipyrimidines were used. For optimization and DFT research, respectively, the 6-311+G(d,p) basis set and B3LYP density functional theory were applied. In all the systems, diphenyl amine moiety acts as the electron-donor component, whereas the nitro/cyano moiety as electron acceptor (anchoring) group. In the conjugated spacer, a methyl/ethyl substituent was used to examine the impact of the auxiliary donor group. The computed HOMO-LUMO gap and the spectral data matched well. The oscillator strength (f), electron injection free energy (ΔG^{inject}) and light-harvesting efficiency (LHE) were also computed and explained. The calculated values for the examined dye-sensitizers open-circuit photo voltage (V_{oc}) and electron coupling constant (V_{RP}) were also included in this research. This study demonstrates that every synthetic dye has promising potential as a dye sensitized solar cells (DSSCs) sensitizer.

Keywords: 2,2′-Bipyrimidine derivatives, DSSCs, Light harvesting efficiency.

INTRODUCTION

New effective and affordable renewable energy sources must be explored in order to produce and meet the demand for electricity without harming the environment. To prevent global warming and improve the production of clean energy with minimal environmental impact, sufficient time must be spent studying the creation of such new resources [1]. In a dye sensitized solar cell (DSSC) device, the dye sensitizers primary jobs are to produce photo-electrons and capture enough light. The dye sensitizers should possess the properties in order to carry out these tasks more effectively depends on the consistency (both physical and chemical), strong adhesion to semiconductors (ETL), a significant amount of incident light absorption (from visible to infrared region) and the eigen values of the HOMO must be less than the E_{redox} of the electrolyte [2-5].

The pyrimidine rings of 2,2′-bipyrimidine contain two nitrogen atoms, which results in the increasing electron affinity [6]. However, when compared to bipyridine, the aromatic ligand has more nitrogen atoms, which reduces the σ-donor strength while increasing the π-acceptor strength [7-9]. The bimetallic complexes are typically electronically linked and 2,2′-bipyrimidine acts as a crucial bridging ligand when the metallic centres are brought together [10]. The energy levels of π-π* orbitals in the basic heterocyclic ligands with a single hetero-atom in an aromatic ring, such as 2,2′-bipyridine, are greater than those of the hetero atoms in an aromatic ring, such as 2,2′-bipyrazine, 2-(2-pyridyl)pyrazine [11]. Thus, these bipyrimdine ligands result in a significant stabilization of the LUMOs and to a lesser extent, of the HOMOs, which causes the red shift absorption. Due to their lower energy π-π* orbitals, they can also be employed to create novel ruthenium(II) dyes and help with improving infrared absorption [11,12]. Additionally, 2,2′-bipyrimidine complexes developed based on the electron donation or withdrawal have been studied and recorded for their capacity for light-harvesting and their applications in the solar energy conversion devices have been well documented.

EXPERIMENTAL

Theoretical background: The investigated dyes electrochemical characteristics in their excited states were confirmed and a trustworthy theoretical framework and the associated results are proposed on its basis in order to qualify the electron

injection into a titanium oxide (TiO_2) surface for few 2,2′-biyrimidine derivatives. The electro-injection's free energy change (eV) is computed as

$$\Delta G^{inject} = E_{ox}^{dye*} - E_{CB}^{TiO_2} \quad (1)$$

where $E_{CB}^{TiO_2}$ and E_{ox}^{dye*} give information on the energy of the conduction band in TiO_2 semiconductor as well as the oxidation potential of dye in its excited state, respectively [13]. Since the pH of the solution and $E_{CB}^{TiO_2}$ is the surface conditions affect the energy of the TiO_2 conduction band, it is exceedingly difficult to obtain the exact value. We use $E_{CB}^{TiO_2} = 4.0$ eV band from the stated values of the various materials for this reason [14]. Based on the presumption that the semiconductor is in contact with aqueous redox electrolytes with a fixed pH, the stated values must be determined experimentally [15]. The electron injection from the material's excited and unrelaxed states can be calculated based on the determination of E_{ox}^{dye*}. The chemical route, which can be described in eqn. 2 will be utilized to determine the excited state oxidation potential.

$$E_{ox}^{dye*} = E_{ox}^{dye} - \lambda_{max}^{ICT} \quad (2)$$

where λ_{max}^{ICT} the photo-induced intermolecular charge transfer and the energy of intermolecular charge transfer and E_{ox}^{dye*} is the ground states, where the redox potential is located.

The efficiency of DSSC can be measured by the dyes response to the incident light. To maximize the photocurrent response, the light harvesting efficiency (LHE) values of dyes must be as high as possible. Eqn. 3 was used to determine the LHE.

$$\text{Light harvesting efficiency (LHE)} = 1 - 10^{-f} \quad (3)$$

where f is the oscillator strength of the dye.

Using the link between V_{oc} and the energy of LUMO (E_{LUMO}) of the dyes based on electron injection from LUMO to the conduction band (E_{CB}) of the semi-conductor TiO_2, it is possible to approximatively estimate the open-circuit photo voltage V_{oc} (eV) [16,17].

$$V_{oc} = E_{LUMO} - E_{CB} \quad (4)$$

The electron coupling constant $|V_{RP}|$ was calculated from ΔG^{inject}, which is represented by the following expression [18]:

$$|V_{RP}| = \frac{\Delta G^{inject}}{2} \quad (5)$$

Computational method: 2,2′-Bipyrimidine and newly designed dyes comprehensive geometry optimizations and the electronic structure computations were initially carried out in vacuum utilizing the B3LYP functional and 6-311+G (d,p) basis set. The studied 2,2′-biyrimidine sensitizers were studied in three solvents *viz.* dimethyl formamide (DMF), dichloromethane (DCM) and trifluoro acetic acid (TFA). The ground state geometries of these sensitizers were optimized using the polarized continuum model (PCM) with larger basis set 6-311+G(d,p) and exact energy minimum frequency calculations were carried out at the same level to Gaussian 09 is the package utilized in the current computation [19]. Frequency calculations were performed using the same degree of theory as geometry optimization of the dyes' ground state in the gas phase. A newly deve-

loped functional, the long-range (B3LYP) approach, introduces long-range interactions by comparing 19% of HF and 81% of B88 exchange at short range with 65% of HF plus 35% of B88 at long range [20]. Additionally, the B3LYP was used to obtain appropriate exciting energies and can forecast excellent absorption spectra [21-28].

RESULTS AND DISCUSSION

Molecular orbitals: In order to achieve the superior photo-induced intramolecular charge transfer efficiency, donor, bridge and acceptor (DBA) moieties are typically present in organic sensitizers. Conjugation between the donor and anchoring groups is necessary for this charge transfer. The present work evaluates and reports the electron transfers studies of newly developed sensitizers with appropriate DBA and derivatives of 2,2′-bipyrimidine molecule (Fig. 1). From the auxiliary donor (AD) to the acceptor (A), the flow of electrons is shown in Fig. 2. For the preparation of more effective dyes for dye-sensitized solar cells, this study will be beneficial to experimental photo-chemists.
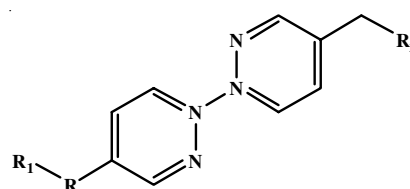
R = $C_{12}H_{11}N$; BPM-1: R_1 = CH_3, R_2 =NO_2; BPM-2: R_1 =C_2H_5, R_2 = NO_2; BPM-3: R_1 = C_2H_5, R_2 = CN; BPM-4: R_1 = CH_3, R_2 = CN

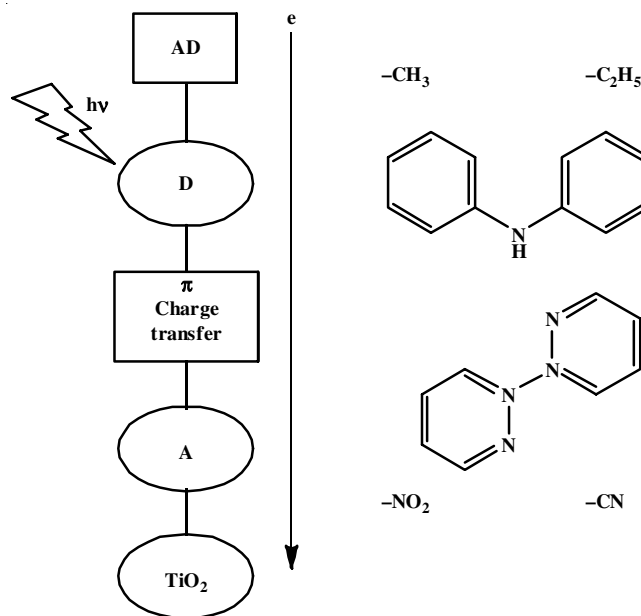Fig. 1. Chemical structures of newly designed dyes

Fig. 2. Different parts of AD-D-π-A system. AD = auxiliary donor, D = donor, π = pi-spacer, A = acceptor

The goal of the current study is to increase the electron injection efficiency of DSSCs using theoretical analysis of structural alterations in 2,2′-bipyrimidine-based dyes. Theoretically, it is feasible to test a sizable panel of novel struc-

tures and determine all the dye alterations. These dyes nitro (-NO$_2$) and cyano (-CN) groups serve as the acceptor units, while the diphenyl moiety serves as a spacer when other substituents are utilized as donors. In DSSCs, I$^-$/I$_3^-$ system is typically utilized as the electrolyte.

The molecular orbital (MO) study was carried out at the B3LYP/6-311+G (d,p) level of theory to get deeper understanding of the molecular structure and electronic distribution of these dyes. Fig. 3 shows the gas phase HOMO and LUMO distribution pattern for dyes based on 2,2′-bipyrimidine at the DFT/B3LYP/6-311+G(d,p) level of theory. Table-1 listed the various determined molecular energy gap values. Fig. 4 also depicts the energy distribution of BPM, BPM-1, BPM-2, BPM-3 and BPM-4 molecules in the gas phase. In light of aforementioned information and taking into account the BPM, BPM-1, BPM-2, BPM-3 and BPM-4 molecular orbital structure, electronic charge transfer from either the acceptor or donor moiety to the π-spacer group by light irradiation results in HOMO → LUMO excitation. The LUMO of BPM-4, which indicates the larger positive value of electron injection free energy in BPM-4, serves as the primary acceptor of 2,2′-bipyrimidine. The cyano group in the bipyrimidine group and the ethyl group dye in

the diphenyl amine moiety appear to be possible sensitizers as a result.

More positive potential LUMO energy is needed for the direct charge transfer from the dye excited state to the TiO$_2$ conduction band than for TiO$_2$ (-4.0 eV). Additionally, the charge regeneration would need more negative HOMO energy than -4.80 eV reduction potential energy of the electrolyte (I$^-$/I$_3^-$), which is required for the decrease of the charge. Fig. 4 shows the energy level diagrams of the HOMO and LUMO for the examined dyes as well as the conduction band energy of TiO$_2$ (at -4.0 eV) and the redox potential energy of electrolyte of gas phase, DMF, DCM and TFA media. Using the PCM model, the HOMO and LUMO energy values of the dyes in the gas phase and in various solvents have been calculated. While the LUMOs energy level of the dyes lies over the conduction band energy of TiO$_2$, the HOMOs energy levels are often lower than the redox potential energy of the electrolyte.

This reflects that TiO$_2$ is compatible with instantaneous charge transfer and charge regeneration, as seen in Fig. 4. This demonstrates that the dyes and derivatives of bipyrimidine can both function as potential light sensitizers. The negative values of HOMO derivatives are greater than those of LUMO deriva-
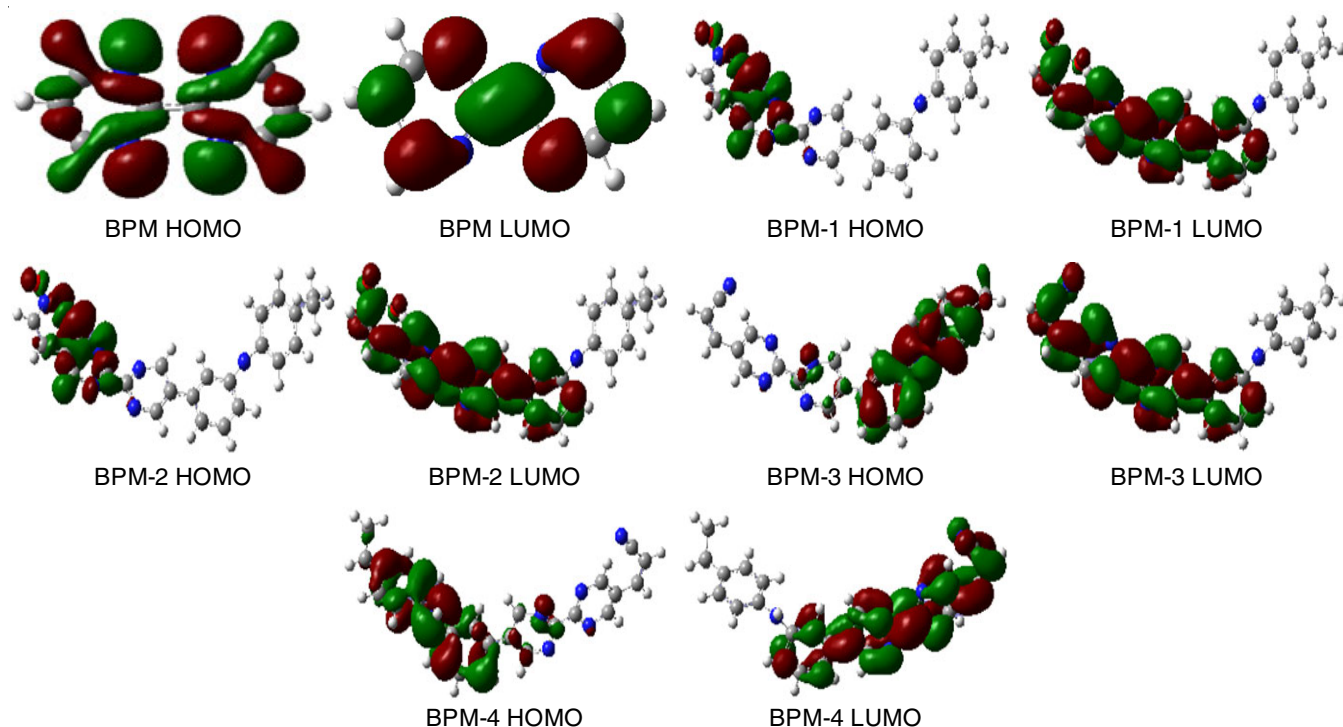

Fig. 3. HOMO and LUMO distribution pattern of 2,2'-bipyrimidine based dyes at DFT/B3LYP/6-311+G(d,p) level of theory in gas phase

Dye	Gas phase			DMF			DCM			TFA		
	HOMO	LUMO	E$_{gap}$	HOMO	LUMO	E$_{gap}$	HOMO	LUMO	E$_{gap}$	HOMO	LUMO	E$_{gap}$
BPM	-6.6456	-2.4381	4.2074	-6.8760	-2.6607	4.2153	-6.8135	-2.6256	4.1878	-6.7988	-2.6172	4.1816
BPM-1	-4.3775	-3.3127	1.0647	-4.5960	-3.5396	1.0563	-4.5810	-3.5263	1.0547	-4.772	-3.5228	1.0544
BPM-2	-4.3778	-3.3132	1.0645	-4.5952	-3.5391	1.0560	-4.5808	-3.5263	1.0544	-4.5772	-3.5230	1.0541
BPM-3	-5.8975	-2.9149	2.9826	-5.8692	-3.0912	2.7780	-5.8630	-3.0613	2.8017	-5.8619	-3.0542	2.8076
BPM-4	-5.8964	-2.9146	2.9818	-5.8700	-3.0923	2.7777	-5.8632	-3.0618	2.8014	-5.8621	-3.0545	2.8076

TABLE-1
E$_{HOMO}$, E$_{LUMO}$ AND ENERGY GAP (E$_{gap}$) OF DYES (eV) AT B3LYP/6-311+G (d,p) LEVEL OF THEORY
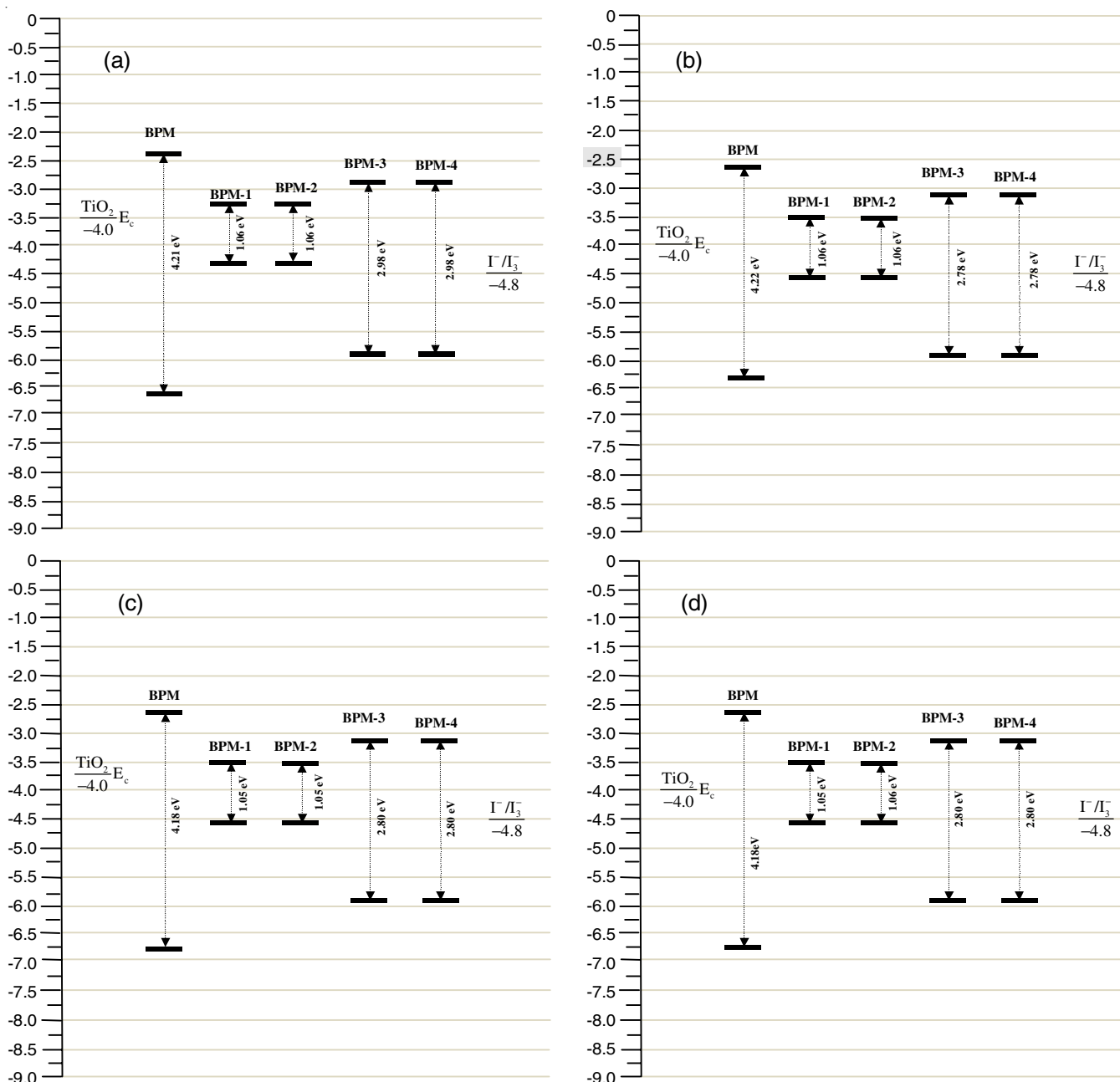
Fig. 4. Schematic energy diagram (E_{HOMO} and E_{LUMO}) of the dyes in (a) gas phase, (b) DMF, (c) DCM and (d) TFA

tives when compared to the neutral levels. Additionally, all of the LUMO levels are present at positions that are identical to the Fermi-level of the semiconductors (ETL). In order to facilitate electron injection from the dye to the active semi-conductor layer, these can be useful and greatly help in the process.

Due to competitive light absorption, the co-adsorbents could easily inject electrons from the co-absorbents into the TiO$_2$ layer I$^-$/I$_3^-$, helping to recover the dip in the dye-based UV spectra near 400 nm. For the DSSC dyes to function properly and more effectively. In order to match the conduction band of TiO$_2$ electrode and the redox energy levels of electrolyte, respectively, we would need suitable LUMO and HOMO energy levels of sensitizers. Higher LUMO values of BPM-1 (-3.3127 eV), BPM-2 (-3.3132 eV), BPM-3 (-2.149 eV) and

BPM-4 (-2.9146 eV) relative to TiO$_2$ conduction band edge better allow the electron injection from the co-adsorbents to the TiO$_2$ film (-4.0 eV). The lower HOMO values of BPM-1, BPM-2, BPM-3 and BPM-4 relative to the redox potential of the co-adsorbents further promote the electron transfer from them. These levels are -4.3775 eV, -4.3778 eV, -5.8975 eV and -5.8964 eV, respectively (-4.80 eV). It is proved by the ongoing study and development that all of the dyes in DMF, DCM and TFA solvents follow the aforementioned trend. In addition to the favourable energy values, the unique orientation of dye is essential for the charge transfer. Because of these features, the rate at which electrons are transported from TiO$_2$ to the oxidized dye becomes slower, and therefore, the power conversion efficiency (PCE) is decreased. The dyes HOMO

should be positioned away from the TiO₂ surface in order to convert energy effectively because that part of the molecule will lack electrons due to its carbocation position. In order for the HOMO to transfer its intramolecular electrical charge to the LUMO upon photo-excitation, the LUMO should be close to the TiO₂ surface. It is significant to observed that all the selected dyes have LUMO energies, which are closed to the TiO₂ surface energy, whereas all 2,2′-bipyrimidine derivatives have HOMO energies that are away from the TiO₂ surface, suggesting that these dyes have potential as DSSC photo sensitizers.

For the dye to work correctly and operate efficiently in a DSSC, the dye sensitizer must have the appropriate LUMO and HOMO energy levels. The redox energy level of electrolyte and the conduction band of TiO₂ electrode should match each other in terms of energy levels. The excited state must be at a higher energy level and have lower electrochemical potential than the TiO₂ conduction band in order to efficiently inject electrons. It is found that the E_{gap} is less in case of 2,2′-bipyrimidine with -NO₂ acceptor and –C₂H₅ donor (BPM-2). The E_{gap} value also decreases as the polarity of the solvent increases. Thus, E_{gap} is the least for BPM-2 in TFA. Additionally, the dye needs to have a higher positive oxidation potential and be at a

lower energy level than the redox electrolyte energy used to regenerate the dye cation after the photoinduced electron injection into TiO₂. The dyes HOMO should be situated away from the TiO₂ surface in order to convert energy effectively because that part of the molecule will lack electrons due to its carbocation location. In order for the HOMO to transmit its intramolecular electrical charge to the LUMO upon photo-excitation, the LUMO should be close to the TiO₂ surface. The LUMO energies of the studied dyes are in close proximity to the TiO₂ surface energy, whereas the HOMO energies of the bipyrimidine derivatives are distant from the TiO₂ surface, suggesting that these dyes may be useful as DSSC light sensitizers.

Optical properties: In order to obtain Fig. 5 the optical property and electronic transition from the excitation energy and the UV/Vis absorption spectra, the singlet-singlet transition of all the sensitized dyes is simulated using DFT with B3LYP functional *in vacuo* and DMF, DCM and TFA solutions. The oscillator strength of each sensitized dye in vacuum and in the solvent media is reported in Table-2 together with all the computed vertical excited singlet states. Fig. 5 shows the investigated substances that reached B3LYP/6-311+G(d,p) values. The position (connected to the distance between the HOMO
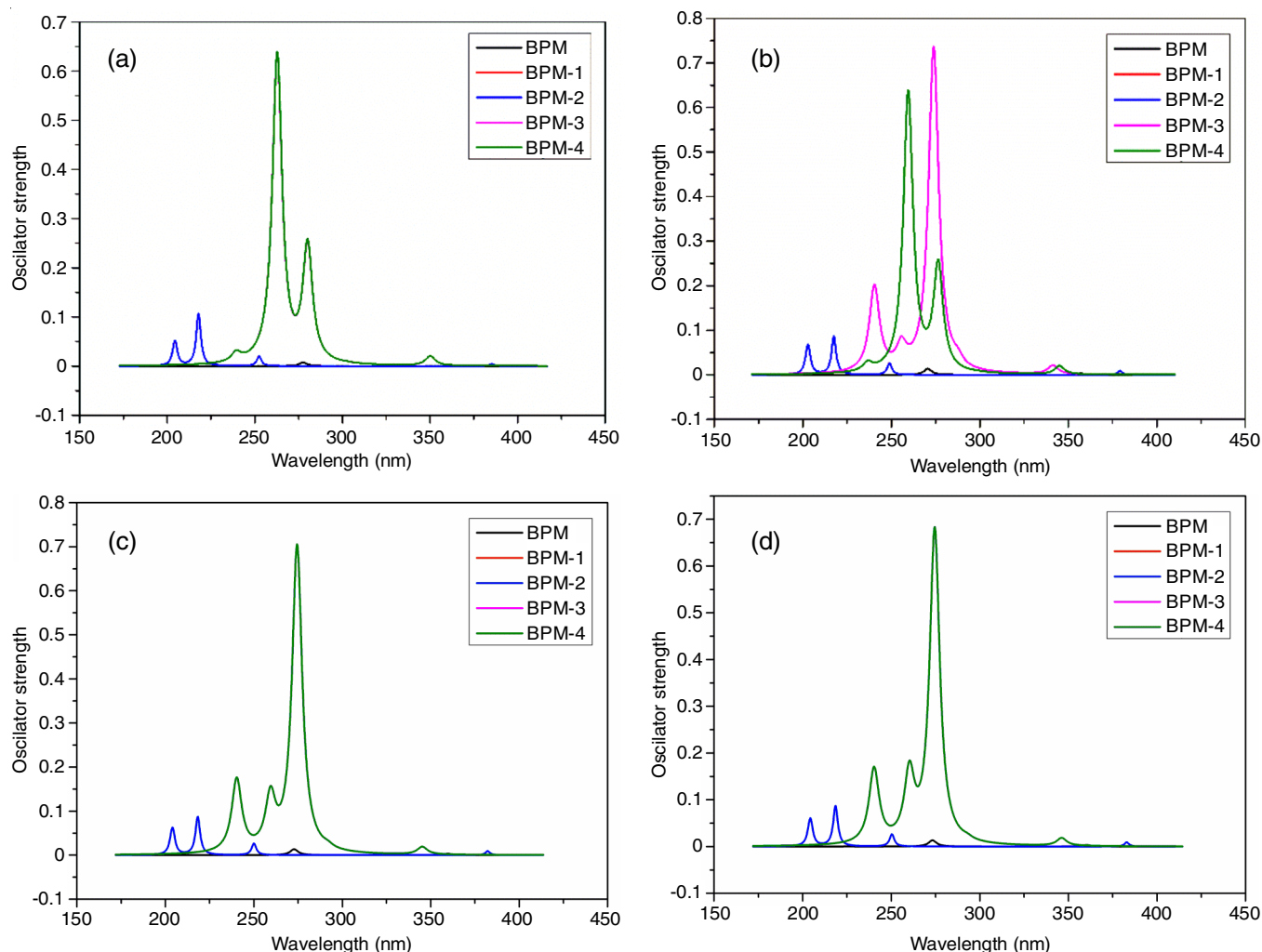

Fig. 5.　Simulated UV-visible absorption spectra of dyes calculated in (a) gas phase (b) DMF (c) DCM (d) TFA at DFT/B3LYP/6-311+G(d,p) level of theory

TABLE-2
LIGHT HARVESTING EFFICIENCY (LHE) AND AVERAGE LIGHT HARVESTING EFFICIENCY (LHE$_{avg}$),
OSCILLATOR STRENGTH (f) ABSORPTION SPECTRA (λ_{max}) OF DYES AT B3LYP/6-311+G(d,p) LEVEL OF THEORY

Dye	λ_{max}	F	LHE	LHE$_{avg}$	λ_{max}	f	LHE	LHE$_{avg}$
	Gas phase				Dimethyl formamide			
BPM	302.26	0.0072	0.0164	0.0085	293.52	0.0124	0.0028	0.0021
	266.05	0.0002	0.0005		260.05	0.0006	0.0014	
BPM-1	685.49	0.0152	0.0344	0.0431	659.24	0.0259	0.0579	0.0372
	513.56	0.0231	0.0518		580.47	0.0072	0.0164	
BPM-2	685.56	0.0153	0.0346	0.0426	659.18	0.0259	0.0579	0.0372
	514.02	0.0225	0.0505		580.61	0.0072	0.0164	
BPM-3	410.31	0.0430	0.0943	0.3986	400.04	0.3049	0.5044	0.5624
	389.58	0.5270	0.7028		392.70	0.4207	0.6204	
BPM-4	410.31	0.0433	0.0949	0.3996	399.99	0.3094	0.5095	0.5649
	389.65	0.5290	0.7042		392.63	0.4206	0.6203	
	Dichloromethane				Trifluoro acetic acid			
BPM	296.12	0.0123	0.0279	0.0147	296.73	0.0121	0.0275	0.0145
	262.25	0.0006	0.0014		262.77	0.0006	0.0014	
BPM-1	655.93	0.0235	0.0527	0.0348	655.17	0.0229	0.0514	0.0342
	578.06	0.0074	0.0169		577.29	0.0074	0.0169	
BPM-2	655.88	0.0236	0.0529	0.0349	655.12	0.0229	0.0514	0.0342
	578.38	0.0074	0.0169		577.65	0.0074	0.0169	
BPM-3	402.10	0.1495	0.2912	0.4303	402.00	0.1184	0.2386	0.3866
	395.17	0.3781	0.5813		395.71	0.3322	0.5346	
BPM-4	402.11	0.1506	0.2930	0.4382	402.03	0.1193	0.2402	0.3883
	395.13	0.3803	0.5834		395.68	0.3339	0.5364	

and LUMO levels) and the breadth of the spectrums first band are the two elements, which run the dyes efficiency since the absorption changes to lower energy levels, which in turn favours the light harvesting process. Oscillator strength is an important factor of the sensitizer because it is related with light harvesting efficiency [29]. As a result, the dyes initial vertical excitation energies (ΔE) would be reported in the following order: BPM > BPM-3 > BPM-4 > BPM-1 and BPM-2. The bathochromic shift that occurs while moving from BPM to BPM-2 is also reflected in this. The spectra of BPM-3 and BPM-4 record a little blue-shift with a reduced decreased oscillator strength compared to BPM due to the hetero atoms electronegativity in the electron donor groups. As these compounds can easily change their HOMO and LUMO levels through systematic change of the donor and acceptor groups and π-conjugated spacer, donor-π-acceptor (D-π-A) type compounds have attracted a significant amount of research attention in recent years.

Table-2 reveals that the spacer group and the kind of the substituent have an impact on the maximum absorption in the dyes under study. A red shift is observed when 2,2′-bipyrimidine moiety is exposed to spacer. Thus BPM has the shortest λ_{max} value. This is due to the ability of the electron-donating group to raise E_{HOMO} but decreasing E_{LUMO}. In the spectral analysis of catechol-based dyes as sensitizers in DSSCs, Ooyama *et al.* reported the similar observations [30]. The presence of an electron-releasing group shifts the absorption maximum of a given acceptor in 2,2′-bipyrimidine group to a longer wavelength. Thus, BPM-4 has longer absorption maximum than those of other dyes. The following characteristics are present in 2,2′-bipyrimidine derivatives structural design in this work: (a) DPA works as a π-conjugated spacer (b) alkyl groups as electron donating moiety (c) 2,2′-bipyrimidine as π-conjugated

heterocyclic system and (d) nitrile and nitro groups as electron acceptors. The absorption spectrum of the photosensitizers should usually cover the visible region spectrum and even some near-infrared wavelengths [31]. These molecules were developed and have significant absorption in the visible band between 400 and 600 nm (visible region) especially in solutions. Due to the spacer DPA, which causes BPM-1 to BPM-4 molecules to be larger than the basic 2,2′-bipyrimidine molecule and its derivatives are suitable for compact monolayer formation by covering the base TiO_2 surface during the dye uptake process. Table-2 shows that the BPM-4 system has high oscillator strength and may have the highest light harvesting efficiency of the tested sensitizers. The simulated spectra show that the characteristics of the spectra of all the dyes are similar.

Intramolecular charge transfer: The intramolecular charge transfer is one of the most important characteristics of the metal-free organic sensitizers present in DSSC function based on donor to acceptor/anchoring group (ICT). The primary contribution of frontier molecular orbital to this behaviour in the dyes (FMO). The HOMO and LUMO orbital spatial distribution of all the 2,2′-bipyrimidine derivatives is shown in Fig. 3. The HOMO and LUMO plots show the typical properties of π-π* type molecular orbitals. Additionally, HOMO exhibits an anti-bonding character between two neighbouring pieces and a bonding character within the units. As a result, the electronic transition of the π-π* kinds correlates with the lowest-lying singlets of LUMOs. Although the qualitative similarities between the HOMO and LUMO patterns end there, the electron distributions are distinct. The electrons in HOMOs are mostly shared between the electron donor and the π-conjugated spacer. Whereas in LUMOs they are positioned on the fragments of the electron acceptor and the conjugation spacer moiety (nitro and nitrile).

Therefore, any electronic transitions from HOMO to LUMO in any D-π-A dye would cause an intramolecular charge transfer from the donor units to the acceptor/anchoring groups *via* the conjugated bridge. As a result, these HOMO-LUMO transitions are categorized as a π-π* ICT. The anchoring group (nitro and nitrile) of the dyes to the LUMOs significantly helped to lead a strong electronic connection on TiO_2 surface, which boosted the electron injection efficiency. Additionally, this gradually increases the J_{sc} (short-circuit current density).

Photovoltaic properties: Ground (E_{ox}^{dye}) and excited (E_{ox}^{dye*}) state oxidation potentials, electronic injection free energy (ΔG^{inject}), open circuit photovoltage (V_{oc}), current density (J_{sc}) and light harvesting energy (LHE) are the principal factors in the design of efficient DSSCs. To maximize the power conversion efficiency, these features have been the focus of numerous studies [32-34]. According to Koopman's theorem, the ground state oxidation potential (E_{ox}^{dye}) for all of these colours is considered to be the negative E_{HOMO} [35]. Eqn. 2 was used to determine the E_{ox}^{dye*} values. The values of the ground state E_{ox}^{dye} and excited state E_{ox}^{dye*} oxidation potentials are shown in Table-3. It can be observed that all dyes E_{ox}^{dye*} are in the order of BPM < BPM-1 < BPM-3 < BPM-2 < BPM-4. It is evident from the values that BPM is the most suitable oxidizing species among the four dyes while BPM-4 is the least suitable one. Eqn. 1 was used to estimate the ΔG^{inject} values for the dyes studied redox reactions. All of these values are negative, indicating the spontaneous nature of the electron injection from dye to TiO_2. Table-3 shows that the ΔG^{inject} calculations are in the following order: BPM-3 > BPM-4 > BPM-2 > BPM-1 > BPM in gas phase and the order for all solvents are BPM-4 > BPM-3 > BPM-1 > BPM-2 > BPM. Further, BPM-4 has the largest ΔG^{inject} value while BPM has the smallest value. The ΔG^{inject} values are influenced by solvent. In more polar solvents like TFA than in less polar DCM, the readings are more negative.

While going from BPM to BPM-1, we can calculate a anodic shift of 2.2681 and 0.0251 eV for E_{ox}^{dye} and E_{ox}^{dye*}, respectively. If we compare the oxidation potentials in gas phase with those in solvents, we found that anodic shift is induced the solvent. Secondly, there is slight anodic shift in the series BPM-4 → BPM-3 → BPM-2 → BPM-1 → BPM in gas phase and corresponding solvents.

The light harvesting efficiency (LHE) value is important to enhance the current density (J_{sc}), which results in increasing efficiency of DSSCs. Table-2 contains the average values of LHE for the dyes. The spectra of other simulated dyes are further extended in the following sequence: BPM < BPM-3 < BPM-4 < BPM-1 < BPM-2, which in turn aligns well with the change trend of the absorption spectra since the LHE spectra of BPM-1, BPM-2 are more red shifted than those of BPM. The BPM-1 to BPM-4 LHE has shown a substantial improvement. The highest absorption intensity is found in BPM-4 with methyl and nitrile. It has been shown that the inclusion of asymmetric auxiliary ligands improves the ability of harvest light of the complex BPM-4. The LHE for all dyes were in the range 0.002-0.56. 2,2′-Bipyrimidine complexes absorption spectra have larger LHE spectra that are well-matched to the spectrum of solar energy. This means that all the sensitizers give similar range of photocurrent. The open circuit voltage is a further important element in the design of DSSCs (V_{oc}).

Table-4 shows the computed V_{oc} values of the dyes, which indicate how much solar energy is converted into electricity [19,36]. It is clear from Table-4 that the potential value varies in between 0.46-1.56 V for the investigated dyes. In case of 2,2′-bipyrimidine based dyes, the V_{oc} values are adequate for a better injection of electrons from E_{LUMO} to the conduction band of TiO_2, which indicates that 2,2′-bipyrimidine derivatives are potential candidates in the design of DSSCs. The coupling constant ($|V_{RP}|$) between the organic dyes and semiconductor surface determines the rate of electron injection (kinetic property) and it may be estimated using eqn. 5. The rate of electron injection will increase as the electron-coupling constant rises. Table-4 lists the computed ($|V_{RP}|$) values for the suggested dyes. Irfan & Muhammad [37] recently investigated the use of the DFT method to modify the structure of solar cell materials to tune their electronic and charge transfer properties. They asserted that ΔG^{inject} and ($|V_{RP}|$) are increased when more activating groups are present in the donor part and more deactivating groups are present in the acceptor part of the sensitizer [35]. In present study, it is observed that BPM-1 contains –CH_3 as group in the donor moiety and –NO_2 group in the acceptor part. Similarly, BPM-4 possess high V_{RP} values with more activating –CH_3 group in donor and –CN as deactivating group. In these

TABLE-3
CALCULATED ABSORPTION SPECTRA λ_{max}, ΔG^{inject}, OXIDATION POTENTIAL, INTRAMOLECULAR CHARGE TRANSFER ENERGY OF DYES AT B3LYP/6-311+G(d,p) LEVEL OF THEORY

Dye	λ_{max}	λ_{max}^{ICT}	E_{ox}^{dye*}	ΔG^{inject}	λ_{max}	λ_{max}^{ICT}	E_{ox}^{dye*}	ΔG^{inject}
	Gas phase				Dimethyl formamide			
BPM	302.26	4.1019	2.5437	-1.4563	293.52	4.2240	2.652	-1.348
BPM-1	685.49	1.8087	2.5688	-1.4312	659.24	1.8807	2.7153	-1.2847
BPM-2	685.56	1.8085	2.5693	-1.4307	659.18	1.8809	2.7143	-1.2857
BPM-3	410.31	3.0217	2.8458	-1.1242	400.04	3.0993	2.7699	-1.2301
BPM-4	410.31	3.0218	2.8746	-1.1254	399.99	3.0997	2.7703	-1.2297
	Dichloromethane				Trifluoro acetic acid			
BPM	296.12	4.1869	2.6266	-1.3734	296.73	4.1784	2.6204	-1.3796
BPM-1	655.93	1.8902	2.6908	-1.3092	655.17	1.8924	2.6848	-1.3152
BPM-2	655.88	1.8904	2.6904	-1.3096	655.12	1.8925	2.6847	-1.3153
BPM-3	402.10	3.0835	2.7795	-1.2205	402.00	3.0842	2.7777	-1.2223
BPM-4	402.11	3.0834	2.7798	-1.2202	402.03	3.0839	2.7782	-1.2218

TABLE-4
ELECTRON COUPLING CONSTANTS ($|V_{RP}|$) AND OPEN-CIRCUIT PHOTO VOLTAGE IN eV (V_{oc}) OF BIPYRAMIDINE DYES

Dye	Gas phase		Dimethyl formamide		Dichloromethane		Trifluoro acetic acid	
	$|V_{RP}|$	V_{oc}	$|V_{RP}|$	V_{oc}	$|V_{RP}|$	V_{oc}	$|V_{RP}|$	V_{oc}
BPM	0.7282	-1.56	0.674	-1.34	0.6867	-1.37	0.6898	-1.38
BPM-1	0.7156	-0.69	0.6424	-0.46	0.6546	-0.47	0.6576	0.58
BPM-2	0.7154	-0.69	0.6429	-0.46	0.6548	-0.47	0.6577	-0.48
BPM-3	0.5621	-1.09	0.6151	-0.91	0.6103	-0.94	0.6112	-0.95
BPM-4	0.5627	-1.09	0.6149	-0.91	0.6101	-0.94	0.6109	-0.95

dyes, therefore, the rate of electron injection is significant. In case of BPM-3, a low value of V_{RP} is also seen, indicating a slow electron injection in this system. The electron injection yield, which in turn depends on the qualitative and quantitative absor-ption qualities of the sensitizer and on a good alignment of the sensitizer LUMO level with the semiconductor, is used by J_{sc} to determine the photocurrent density under short circuit conditions. Dye BPM-3 shows a comparatively increased value in both gaseous and corresponding solvents in derivatives of 2,2′-bipyrimidine. It might produce a J_{sc} with a good short-circuit current density. The efficiency of solar energy conver-sion is limited by excessive regeneration energy, which also causes reduced V_{oc}.

Conclusion

This study examines the electrical and optical absorption characteristics of 2,2′-bipyrimidine based organic dyes with conjugated spacers (DPA) in order to evaluate their potential use in dye sensitized solar cells (DSSCs). These compounds include diphenylamine spacer group along with an electron donor moiety composed of methyl, ethyl and amino groups. Nitrile/nitro group serves as the acceptor and anchor for the bipyrimidine group. These dyes calculated E_{HOMO} and E_{LUMO} values are pres-ented for the gas phase and three solvents. The effectiveness of sensitizers in the DSSC systems is discussed based on essential preferred electrical and optical features and light harvesting efficiency. The proposed photo-sensitizers ΔG^{inject} and LHE were improved by the electron donor groups in the diphenylamine moiety and electron acceptor groups in the bipyrimidine. The computed values for ΔG^{inject}, V_{RP} and V_{oc} indicate that these dyes have a high potential for application as photo-sensitizers in DSSCs. The sensitizers thermodynamic and kinetic properties point to the possibility of using these systems as effective photosensitizers in DSSCs. The higher short-circuit current density was the result of all the proposed dyes having strong electron injection driving forces. It is suggested that the developed metal-free organic dyes are the promising options, which could increase the DSSCs power conversion efficiency.

REFERENCES

1. K. Portillo-Cortez, A. Martínez, A. Dutt and G. Santana, *J. Phys. Chem. A*, **123**, 10930 (2019);
https://doi.org/10.1021/acs.jpca.9b09024

2. L.W.A. Vallejo, S.C.A. Quiñones and S.J.A. Hernandez, eds.: L.A. Kosyachenko, The Chemistry and Physics of Dye-Sensitized Solar Cells. In Solar Cell Dye-Sensitized Devices, IntechOpen: Rijeka, Croatia, pp. 399-418 (2011).

3. H. Kusama and K. Sayama, *J. Phys. Chem. C*, **116**, 1493 (2012);
https://doi.org/10.1021/jp208462a

4. S. Rackauskas, N. Barbero, C. Barolo and G. Viscardi, Eds.: K. Maaz, ZnO Nanowires for Dye Sensitized Solar Cells; In Nanowires New-Insights, IntechOpen: Rijeka, Croatia, pp. 59-78 (2017);
https://doi.org/10.5772/67616

5. L.-N. Yang, S.-C. Li, Z.-S. Li and Q.-S. Li, *RSC Adv.*, **5**, 25079 (2015);
https://doi.org/10.1039/C5RA00587F

6. Q. Lin, X. Huang, S. Ramachandran, R. Boonsin, Y. Khendriche, X. Wang, R. Valleix, J.-P. Roblin, D. Boyer, G. Chadeyron and G. Zucchi, *ACS Appl. Polym. Mater.*, **2**, 5581 (2020);
https://doi.org/10.1021/acsapm.0c00915

7. K.Y. Chen, P.A. Schauer, B.O. Patrick and C.P. Berlinguette, *Dalton Trans.*, **47**, 11942 (2018);
https://doi.org/10.1039/C8DT01921E

8. E.V. Dose and L.J. Wilson, *Inorg. Chem.*, **17**, 2660 (1978);
https://doi.org/10.1021/ic50187a056

9. S. Ernst and W. Kaim, *J. Am. Chem. Soc.*, **108**, 3578 (1986);
https://doi.org/10.1021/ja00273a005

10. J. Zhang, Y. Liu and P. Yu, *J. Chin. Chem. Soc.*, **66**, 286 (2018);
https://doi.org/10.1002/jccs.201800286

11. H. Ozawa, H. Kawaguchi, Y. Okuyama and H. Arakawa, *Eur. J. Inorg. Chem.*, **2013**, 5187 (2013);
https://doi.org/10.1002/ejic.201300345

12. M.R.E. da Silva, T. Auvray and G.S. Hanan, *Inorg. Chim. Acta*, **499**, 119194 (2019);
https://doi.org/10.1016/j.ica.2019.119194

13. R. Katoh, A. Furube, T. Yoshihara, K. Hara, G. Fujihashi, S. Takano, S. Murata, H. Arakawa and M. Tachiya, *J. Phys. Chem. B*, **108**, 4818 (2004);
https://doi.org/10.1021/jp031260g

14. J.B. Asbury, Y.-Q. Wang, E. Hao, H.N. Ghosh and T. Lian, *Res. Chem. Intermed.*, **27**, 393 (2001);
https://doi.org/10.1163/156856701104202255

15. A. Hagfeldt and M. Graetzel, *Chem. Rev.*, **95**, 49 (1995);
https://doi.org/10.1021/cr00033a003

16. Z.-G. Zhang, J. Min, S. Zhang, J. Zhang, M. Zhang and Y. Li, *Chem. Commun.*, **47**, 9474 (2011);
https://doi.org/10.1039/c1cc13477a

17. Z. Cai-Rong, L. Zi-Jiang, C. Yu-Hong, C. Hong-Shan, W. You-Zhi and Y. Li-Hua, *J. Mol. Struct.*, **899**, 86 (2009);
https://doi.org/10.1016/j.theochem.2008.12.015

18. J.M. Juma, S.A. Vuai and N.S. Babu, *Int. J. Photoenergy*, **2019**, 4616198 (2019);
https://doi.org/10.1155/2019/4616198

19. W. Sang-aroon, S. Saekow and V. Amornkitbamrung, *J. Photochem. Photobiol. Chem.*, **236**, 35 (2012);
https://doi.org/10.1016/j.jphotochem.2012.03.014

20. A.D. Becke, *J. Chem. Phys.*, **98**, 1372 (1993);
https://doi.org/10.1063/1.464304

21. A.D. Becke, *Phys. Rev. A Gen. Phys.*, **38**, 3098 (1988);
https://doi.org/10.1103/PhysRevA.38.3098

22. C. Lee, W. Yang and R.G. Parr, *Phys. Rev. B Condens. Matter*, **37**, 785 (1988);
https://doi.org/10.1103/PhysRevB.37.785

23. R.J. Magyar and S. Tretiak, *J. Chem. Theor. Comput.*, **3**, 976 (2007);
https://doi.org/10.1021/ct600282k

24. T. Yanai, D.P. Tew and N.C. Handy, *Chem. Phys. Lett.*, **393**, 51 (2004); https://doi.org/10.1016/j.cplett.2004.06.011

25. Y. Xue, L. An, Y. Zheng, L. Zhang, X. Gong, Y. Qian and Y. Liu, *Comput. Theor. Chem.*, **981**, 90 (2012); https://doi.org/10.1016/j.comptc.2011.11.050

26. A.W. Lange, M.A. Rohrdanz and J.M. Herbert, *J. Phys. Chem. B*, **112**, 6304 (2008); https://doi.org/10.1021/jp802058k

27. M.A. Rohrdanz and J.M. Herbert, *J. Chem. Phys.*, **129**, 034107 (2008); https://doi.org/10.1063/1.2954017

28. J. Toulouse, F. Colonna and A. Savin, *J. Chem. Phys.*, **122**, 014110 (2005); https://doi.org/10.1063/1.1824896

29. X. Li, P. Song, D. Zhao and Y. Li, *Materials*, **13**, 4834 (2020); https://doi.org/10.3390/ma13214834

30. Y. Ooyama, M. Kanda, K. Uenaka and J. Ohshita, *ChemPhysChem*, **16**, 3049 (2015); https://doi.org/10.1002/cphc.201500419

31. K. Moneer, L. Mohsen, R. Marwa and J.H. Fraih, *J. Glob. Pharma Technol.*, **12**, 206 (2017).

32. K. Kakiage, H. Osada, Y. Aoyama, T. Yano, K. Oya, S. Iwamoto, J. Fujisawa and M. Hanaya, *Sci. Rep.*, **6**, 35888 (2016); https://doi.org/10.1038/srep35888

33. L. Etgar, G. Schuchardt, D. Costenaro, F. Carniato, S.M. Zakeeruddin, C. Bisio, M.K. Nazeeruddin, L. Marchese and M. Graetzel, *J. Mater. Chem. A Mater. Energy Sustain.*, **1**, 10142 (2013); https://doi.org/10.1039/c3ta11436h

34. Z. Liu, L. Krückemeier, B. Krogmeier, B. Klingebiel, J.A. Márquez, S. Levcenko, S. Öz, S. Mathur, U. Rau, T. Unold and T. Kirchartz, *ACS Energy Lett.*, **4**, 110 (2019); https://doi.org/10.1021/acsenergylett.8b01906

35. R.G. Pearson, *Inorg. Chem.*, **27**, 734 (1988); https://doi.org/10.1021/ic00277a030

36. H. Wang, Y. Li, P. Song, F. Ma and Q. Wang, *Mol. Phys.*, **114**, 3518 (2016); https://doi.org/10.1080/00268976.2016.1244357

37. A. Irfan and S. Muhammad, *Int. J. Electrochem. Sci.*, **10**, 3600 (2015).